

SecurePose: Automated Face Blurring and Human Movement Kinematics Extraction from Videos Recorded in Clinical Settings

Rishabh Bajpai, *Graduate Student Member, IEEE*, and Bhooma Aravamathan

Abstract—Movement disorders are typically diagnosed by consensus-based expert evaluation of clinically acquired patient videos. However, such broad sharing of patient videos poses risks to patient privacy. Face blurring can be used to de-identify videos, but this process is often manual and time-consuming. Available automated face blurring techniques are subject to either excessive, inconsistent, or insufficient facial blurring – all of which can be disastrous for video assessment and patient privacy. Furthermore, assessing movement disorders in these videos is often subjective. The extraction of quantifiable kinematic features can help inform movement disorder assessment in these videos, but existing methods to do this are prone to errors if using pre-blurred videos. We have developed an open-source software called SecurePose that can both achieve reliable face blurring and automated kinematic extraction in patient videos recorded in a clinic setting using an iPad. This software, extracts kinematics using a pose estimation method (OpenPose), tracks and uniquely identifies all individuals in the video, identifies the patient, and performs face blurring. The software was validated on gait videos recorded in outpatient clinic visits of 116 children with cerebral palsy. The validation involved assessing intermediate steps of kinematics extraction and face blurring with manual blurring (ground truth). In addition, when SecurePose was compared with six selected existing methods, it outperformed other methods in automated face detection and achieved ceiling accuracy in 91.08% less time than a robust manual face blurring method. Furthermore, ten experienced researchers found SecurePose easy to learn and use, as evidenced by the System Usability Scale. The results of this work validated the performance and usability of SecurePose on clinically recorded gait videos for face blurring and kinematics extraction.

Index Terms—Face blurring, patient data anonymization, automation, software development

I. INTRODUCTION

BROAD sharing of anonymized medical data has the potential to dramatically optimize clinical care and clinical research. For example, the lack of large volumes of reliably acquired and anonymized training data is restricting healthcare from fully leveraging the capabilities of Artificial Intelligence (AI) to facilitate clinical assessment. In addition, as medical decision-making becomes more complex, there is increasing value for consensus-based assessment of patient data and improving the accessibility to unbiased quantifiable analogues of subjective physician assessment. Therefore, there is an urgent need to improve protected medical data-sharing techniques and create clinically feasible methods to extract quantifiable and

clinically valuable metrics from these data that can aid clinical decision-making. Video recordings from clinical visits play a crucial role in screening for many disorders and tracking the effects of treatments. This is particularly true for motor disorders, which utilize several video-based or video-assisted assessments ([1]–[4]).

Additionally, video data sharing facilitates research endeavors, allowing researchers to access a larger pool of diverse patient data, which enhances the generalizability and statistical power of studies. However, it is critical to follow patient-sensitive data-sharing guidelines to anonymize the data before sharing. Despite the existence of numerous regulations, there is a lack of practical guidance on how to effectively share such data while simultaneously ensuring the confidentiality of participants. Laws such as the Health Insurance Portability and Accountability Act (HIPAA) [5] in the United States, the General Data Protection Regulation (GDPR) [6] in the European Union, and the Personal Data Protection Bill (PDPB) [7] in India emphasize the protection of data containing full-face images as sensitive personal identifiers. Therefore, for de-identifying video data, any information such as the face and name of a patient that can be used to identify the patient should be removed before storing it on a non-local server. Despite increased funding for medical research and improved medical infrastructure for data sharing, patient video data anonymization remains a challenge for researchers due to the extensive time required for manual face blurring.

Research-based assessment of these video recordings, including many newly available open-source pose-estimation tools ([8]–[12]), can be useful for quantifying motor disorders that were previously only subjectively assessed. Kinematics data extracted from video recordings can aid the understanding of motor disorders and inform the development of automated tools for accurate quantification of the movements seen with these disorders. However, extracting body kinematics using current pose estimation algorithms on de-identified videos (face-blurred) may result in less accurate kinematics, and thus may not be suitable for movement assessment [13]. Therefore, to best facilitate the clinical and research-based assessment of motor disorders, we need a reliable methodology to automatically extract body kinematics from video recordings followed by patient de-identification (e.g., face blurring) on a local server. This will allow for reliable kinematics extraction while also facilitating secure sharing of videos across centers.

R. Bajpai and B. Aravamathan are with the Department of Neurology, Washington University in St. Louis, USA. E-mail: (bajpai@wustl.edu and rishabhajpai24@gmail.com) and aravamathanb@wustl.edu

A. Literature review

The literature review focused on face detection and the effect of face blurring on kinematics extraction.

1) *Face Detection* : The first step in automated face blurring is to detect the faces in the video. Most face detection methods are trained to detect faces in images, so they perform face detection frame-by-frame in a video. Face blurring in videos differs from face blurring in images due to the added temporal aspect of videos. In images, only spatial information is available for detecting and blurring faces. In videos, a blurring algorithm can consider the spatial-temporal continuity of individuals across multiple frames to improve face detection and blurring. However, handling multiple frames also presents challenges in achieving consistent and smooth blurring to ensure the subject's anonymity throughout the video. Additionally, any tracking or association algorithms used in video face blurring must maintain the consistency of the blurring effect across frames, taking into account variations in pose, motion, and illumination, which are more common in video data collected during clinical care. Our literature review has revealed the unavailability of a clinically relevant face blurring algorithm that guarantees patient privacy protection. The studies discussed in the literature review used various metrics to evaluate their methods' performance. However, for clinical applications, the face blurring technique must be validated using clinically-acquired videos and must accurately blur faces in 100% of frames to ensure patient privacy.

The existing literature using these algorithms for face detection and blurring is summarized below. Notably, the applications of these methods share some common weaknesses: 1) the algorithms are all designed for face detection in images, not video. 2) no applications have validated these algorithms for face detection in clinically acquired video data sets. 3) no applications have demonstrated 100% accuracy for face detection, which is critical to ensure patient privacy for clinical purposes [14]–[16].

Broadly, face detection approaches can be divided into two categories: feature-based approach and image-based approach.

Feature-based approaches

The feature-based approaches extract pre-defined features such as edges, RGB values and corners from the image and use them to find the position and size of the face. The feature-based approaches can be divided into three subcategories namely, active shape model [17]–[21], low-level analysis [22]–[25], and feature analysis [26]–[30]. Among these methods, the Viola-Jones (VJ) [31] algorithm and the Histogram of Oriented Gradients (HOG) [32] are two of the most widely used algorithms.

The VJ algorithm is one of the early successes in face detection proposed by Paul Viola and Michael Jones in 2001, known for its effectiveness in detecting front-facing faces with minimal pose variations. It uses integral images to identify Haar-like features, such as edge features and line features, with a particular focus on features related to the nose and eyebrows. Training of the VJ algorithm involves the use of the Adaptive Boosting (AdaBoost) algorithm to train a detector and cascade filtering which improves both speed and accuracy. This approach is lightweight, achieving a 95 percent detection

rate at 2 frames per second. However, its accuracy can be affected by variations in facial orientation and pose. According to the original paper on VJ, the method becomes unreliable when the face tilt is more than 15 degrees and fails when the face is significantly occluded (especially when the eyes are occluded). Recent works from Alexandre Devaux et al., [33], Karla Brkić et al., [34], Zihao Liu et al., [35] and Farah Saad Al-Mukhtar [36] also found similar challenges while using the VJ for face detection. Alexandre Devaux et al.'s [33] approach obtained a true positives rate of 86.2% with a false detection of 2 faces per image on their dataset. This suggests that the Viola-Jones method may require significant manual efforts to accurately detect faces.

Another popular method, the HOG, known for its high performance in object detection tasks, is also used for face detection due to its faster and less complex computations compared to the VJ [37]. The HOG belongs to the family of image feature descriptors, and it is used to capture the distribution of gradient orientations within localized image regions. Recent studies [38], [39] showed that the HOG-based approaches obtained highest face detection performance among the other feature-based methods including the VJ. However, these studies also showed the HOG-based face detection struggles when faced with scenarios involving faces at unusual angles, obscured facial regions and dark skin-colored faces [38], [39].

Image-based approaches

In comparison to feature-based approaches, most image-based approaches are more robust in real-world applications. Many image-based face detection techniques employ a window-based scanning approach, where a window is moved pixel by pixel to classify faces and non-faces. Each method in image-based approaches differs in terms of the scanning window, step size, iteration number, and sub-sampling rate to enhance efficiency. Image-based approaches are categorized into three main fields: neural networks [40]–[44], linear subspace methods [45]–[49], and statistical approaches [26], [27], [50]–[52]. Face detection algorithms based on convolutional neural networks are known for their accuracy, speed, and exceptional robustness in comparison to linear subspace methods and statistical approaches [16].

Leading models such as the Max Margin Object Detection (MMOD) [53], Multi-task Cascaded Convolutional Neural Networks (MTCNN) [54], and newer neural network models can effectively be utilized to detect faces in diverse and unconstrained environments. In the original the MMOD paper [53], the MMOD outperformed the VJ and the HOG for face detection [55]. However, the MMOD failed to perform well when tested on datasets that included images of faces at different angles, faces of different scales, images with low illumination, and occluded faces [56], [57].

The MTCNN [54] introduced in 2016 showed remarkable performance for face detection and became one of the widely used face detection algorithms. The MTCNN uses a cascaded structure with three stages of carefully designed deep convolutional networks that predict face and landmark locations in a coarse-to-fine manner. The MTCNN [54] surpassed the face detection performances of other contemporary methods on two

data sets (FDDP and WIDER FACE).

Later, several studies used the MTCNN for face detection in face blurring applications. Jizhe Zhou et al., [58] used the MTCNN for face detection, and a modified clustering algorithm for face tracking on a video dataset. Their method obtained an average f1-score of 0.88 for face blurring. TaeMi Park et al., [59] also used the MTCNN for face detection but did not report the face detection performance. A similar approach was used by Yiyang Su and Xiaoming Liu [60], to blur the faces in a front-view gait dataset. A recent study [61] underscores that the MTCNN imposes added computational overhead and overlooks the inherent link between facial landmark localization and bounding box regression. In general, research utilizing the MTCNN has revealed that it is computationally intensive, time-consuming, and requires extensive data for training, rendering it less suitable for real-time applications and video data processing.

Later, several studies used the MTCNN for face detection in face blurring applications, some reporting good face blurring [58], and others not commenting on face detection or blurring performance [59]. A recent study [61] underscores that the MTCNN imposes added computational overhead compared to the VJ and overlooks the inherent link between facial landmark localization and bounding box regression. In general, research utilizing the MTCNN has revealed that it is computationally intensive, time-consuming, and requires extensive data for training, rendering it less suitable for real-time applications and video data processing.

Neural network models like Faster R-CNN [62], Single Shot MultiBox Detector (SSD) [63], and YOLO [64] have become increasingly popular for face detection in recent years. YOLO, in particular, has gained acclaim due to its exceptional performance (57.9 average precision) and swift computations. It employs a one-stage object detection architecture, enabling precise real-time object detection systems. Recently, a YOLOv3-based model (YOLO-face [65]) was trained on WIDER FACE and the Fddb datasets for improved face detection. During the time of model development, YOLO face outperformed other models [64].

Another study [66] compared the face detection performance of eight algorithms, including S3FD [67], Supervised STN [68], YOLO [64], TinyFaces [69], Faceness-net [70], DP2MFD [71], FCN cascade [72], and headhunter [73], by benchmarking their performance on the Fddb dataset. S3FD was found to be better than other algorithms. A similar trend was observed in the original paper describing S3FD [67] where it demonstrated a mean area under the receiver operating characteristic curve of 92.4 on face detection datasets. While YOLO-face and S3FD are considered some of the top algorithms for face detection, their face detection performance decreases when using data sets they were not trained on. This decreased face detection performance manifests as elevated false positives and false negatives. False positives lead to unwanted blurring, make the blurring look unprofessional and sometimes lead to loss of information needed for further analyses. False negatives are even more problematic as the patient's identity remains intact in the video.

2) *Kinematics extraction after face blurring*: The literature on pose estimation indicates OpenPose to be one of the best-performing pose estimation algorithms in everyday tasks [8], [74], [75]. However, using a pose estimation algorithm to extract body kinematics after blurring the faces in the video may result in erroneous kinematic extraction [13].

Whether extracting 2D body kinematics with OpenPose [76] or using 3D motion capture [13], there were more kinematics estimation errors observed when using face-blurred videos compared to unblurred ones. However, there is disagreement within the studies regarding the magnitude of these errors. Bingquan et al. [76] found the errors to be significant, while Jindong et al. [13] found the average errors to be within the acceptable range (less than 1°). Therefore, it is crucial to understand the effect of face blurring on body kinematic extraction and develop a pipeline to effectively extract body kinematics and perform face blurring in patient videos.

B. Motivation and contribution

Automated face blurring and human kinematic extraction are essential for advancing research in diagnosing and studying motor disorders. Existing face detection methods have decreased performance in real-world practical scenarios, particularly when faced with variations in pose, motion, illumination, and unfamiliar data. Maintaining low false positive and false negative rates still remains a challenge in face detection [77]. Even a method with 99% sensitivity may miss blurring the patient's face in 36 frames in a short video of one minute recorded at 60 frames per second (fps). Moreover, manually detecting the missed frame by an automated algorithm is a tedious and erroneous process; human observers may easily overlook detected faces in frames. Any error in face detection, even in a single frame, may expose patient identity.

Due to the above-mentioned limitations of automated face detection methods for face blurring, clinicians and researchers have to use manual face blurring techniques to ensure proper data anonymization. Manual face blurring poses many practical challenges as it requires significant time, effort and manpower. Therefore, there is a need for an accurate and dedicated tool for automated face blurring of patient video data. Additionally, the tool should be able to automatically extract body kinematics that are accurate regardless of face blurring. Key contributions of the work are:

- Automatic identification of the patient and non-patients in the video. This allows users to selectively blur faces and extract patient-specific body kinematics, something existing pose-estimation algorithms are not inherently able to do. These innovations create a novel face blurring scheme for data anonymization and body kinematics extraction.
- An automated pipeline for extracting full-body patient kinematics from videos recorded in clinical settings.
- The first (to the best of our knowledge) open-source graphical user interface (GUI) named SecurePose [78], [79], dedicated to patient kinematics extraction and anonymization of video data. For clinical and research grade face blurring, the GUI also allows the users to de-blur and blur sections of the videos.

- Validation of the SecurePose and comparison with face blurring done using existing face detection algorithms using a clinically-acquired video dataset.

II. METHODOLOGY

A. Dataset description

An ethical approval from the Washington University in St. Louis institutional review board (approval number 202102101) was obtained. In order to utilize their clinical data, including videos, for research purposes, all participants (and caregivers for minors) provided written consent. Between January 1, 2020, and November 4, 2021, participants were recruited from the St. Louis Children’s Hospital Cerebral Palsy Clinic. 180 individuals met study inclusion criteria: age 10 to 20 years old at the time of evaluation, diagnosed with cerebral palsy (per the 2006 consensus diagnostic criteria [80]), have spasticity, and independently ambulatory (classified as levels I-III on the Gross Motor Function Classification System [81]). The age range of 10 to 20 years was selected as it is a period when gait patterns tend to approach maturity and when gross motor function stabilizes in children with cerebral palsy [82]. Out of the initial 180 eligible individuals, 64 individuals were excluded from further analysis because they did not have gait videos that clearly showed the whole body, including the feet. As a result, a total of 116 participants (producing a total of 116 gait videos) fulfilled the inclusion and exclusion criteria and were included for subsequent analysis.

B. Protocol and data collection

A standard gait data collection protocol was used to test the practical applicability of SecurePose in clinical settings. The participants were asked to walk a distance of 15 feet in a straight line on a clinic hallway towards a camera. For video recording, an Apple iPad A1432 with the standard settings of 30 fps and 640x360 pixels resolution were used. In line with real-world recording practices, the camera was not fixed on a tripod but was instead handheld by the clinic staff as they recorded videos. This approach generated practical challenges to clinical video analysis, including motion blur, variable focus, lighting changes and video shaking. Therefore, SecurePose was developed using clinical dataset.

C. Overview of the software design

Pre-processing the videos to prime them for analysis (e.g., standardizing metadata and video orientation), blurring the faces, managing and sharing the anonymized data, and extracting movement kinematics accurately are necessary first steps for clinical movement data processing. The logic flow diagram of SecurePose used to automate these tasks is shown in Fig. 1. The key details of these individual tasks are presented in the following sections. SecurePose is written in Python and its GUI is developed using TKinter [83]. The hardware and software requirements of SecurePose are discussed in its SourceForge repository [78]. In this work, two libraries, namely openHKV (open human kinematics vision) and splib (secure pose library), were developed and used to organize the functions, classes and variables.

D. Project info and meta data

The first screen of SecurePose allows users to enter project information and meta data of the patients. To start the process, the user is asked to either load a previous project or to create a new project by giving it a unique name, select the videos to process, select the directories of the output data and select the meta data of the patients (optional). The software allows users to process multiple videos simultaneously for kinematic extraction and face blurring. The meta data can be in any format and can contain any non-identifiable information, given that it shares the same file names and different file extensions as the videos. For example, for a video named “12345.mp4”, the file containing meta data can have name “12345.xlsx” or “12345.mp3”. SecurePose automatically links the videos with its corresponding meta data by matching file names. Once the project information is entered, a project configuration and log files are created in a newly created project information directory (located within the main SecurePose directory). The project configuration file contains all project-related information and is created using the Python pickle library [84]. This file gets loaded into the workspace whenever the user opens a previously constructed project.

E. Pre-processing: video standardization

Videos recorded from different devices such as mobile phones, tablets and cameras can have different hardware biases and video properties. These inconsistencies in file format and video properties could be problematic for body kinematic and face detection algorithms. To solve this problem, SecurePose automatically scans and standardizes all the videos in the project to ensure shared video properties and removed hardware biases. The video standardization done by SecurePose includes correction of video orientation, resolution, file extension, and audio subtraction (i.e. allows the user to mute the video). To perform the video standardization, a custom script, and modules of the Exiftool and OpenCV libraries were used.

F. Body key point extraction

After pre-processing the videos, the videos are fed into the Windows implementation of OpenPose to extract the coordinates of 25 body key points (shown in Fig. 2) as discussed in the original paper describing OpenPose [8]. OpenPose is utilized in this work over other pose estimation modules because of its high performance for human pose estimation and its inclusion of clinically relevant body key points. At every frame of each video, OpenPose provides the two-dimensional (2D) coordinates of body key points along with a confidence level ranging from 0 to 1. This confidence level represents the algorithm’s level of certainty regarding the accuracy of the key point’s position (coordinates). Since the “BODY 25” model of OpenPose is more accurate and faster than other OpenPose models and also labels foot key points, the BODY 25 model was used in SecurePose. The default resolution settings of OpenPose were used to avoid “out-of-memory” errors during key point extraction. The extracted body key points (output from OpenPose) were stored separately for each frame in

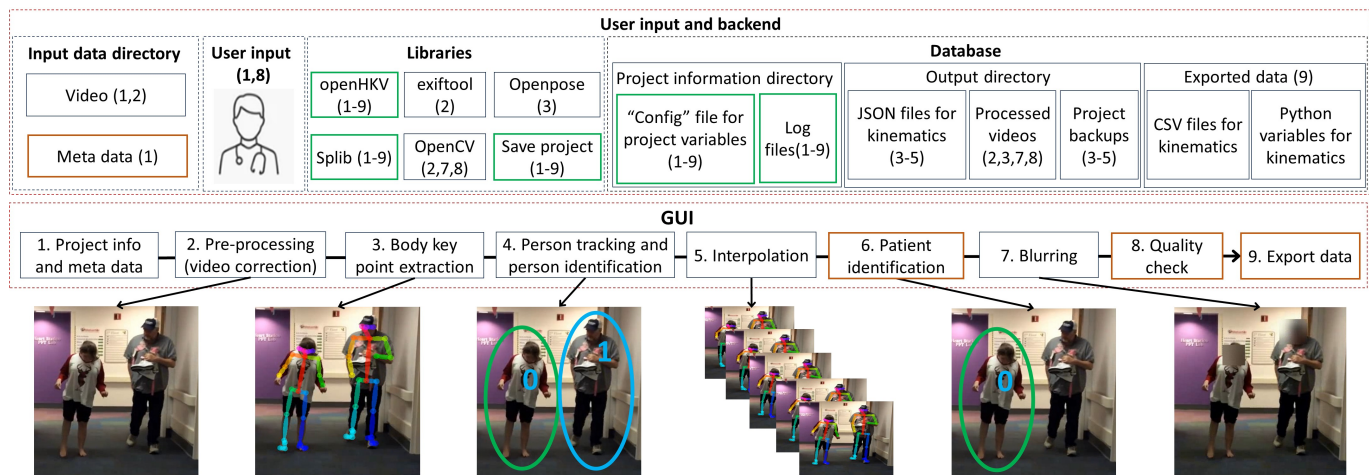


Fig. 1. Logic flow diagram of SecurePose and pictorial representation of some intermediate steps used by SecurePose. The green-colored boundary box modules are called during the execution of each step. The orange-colored boundary box modules are optional steps. Each “GUI” element represents each of 9 steps taken by SecurePose to perform blurring and kinematics extraction. “Input and backend” elements are used by SecurePose for input, processing, and output during these 9 steps, as is indicated parenthetically. For example, “Video” is used during the execution of steps 1 and 2, which are “Project info and metadata” and “Pre-processing (video correction)”.

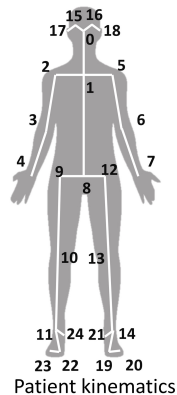


Fig. 2. The index value and location of body key points with respect to the human body.

JavaScript Object Notation (JSON) files format. The GUI of SecurePose allows users to save the OpenPose output videos rendered with extracted body key points to a local directory and visualize the kinematics extraction in real-time.

G. Person tracking and person identification

OpenPose extracts the body key points frame-by-frame from the videos but does not provide any information about how these body key points are related to each other across the frames. Therefore OpenPose can not track the key prints of a single person across the videos. To solve this problem, a custom algorithm was written in Python to identify people in the video and assign a unique ID to each of them by observing their movements (as shown in Fig. 3). The algorithm traverses through all the video frames (JSON files) and iterates over each OpenPose-detected person in the frames. During the traversal, the algorithm keeps track of the movement of the centroids of each person in the video while simultaneously assigning unique IDs to every new person who emerges in a

frame while maintaining existing unique IDs for extant people in the frame. Individual people are tracked by calculating the distance of the person’s centroid to the averaged centroid of people in the previous five frames. Also, the algorithm updates the JSON files by adding unique IDs to the extracted body key points. By the end of this step, every person in the video gets their own unique ID. The reason SecurePose uses this simple approach for tracking people in the video is to reduce computation time and complexity. This algorithm assumes that the centroids of the patient and non-patients do not collide. This assumption is valid in most clinically relevant applications where the clinical staff do not cross over the patient during a video recording session. Since the key-point detection from OpenPose can have missing or erroneous values in some frames, the average of the centroid values for an individual could provide a better estimate of their position. However, taking the average of centroid values across frames may fail to represent fast position changes. Therefore, it is best to track an individual relative to their average centroid over a relatively short time span. We chose to compare an individual’s centroid to their averaged centroid across the last 5 frames noting that the videos in our dataset were recorded at 30 fps.

H. Interpolation

The key point coordinates extracted by OpenPose can be sometimes erroneous or undetected. It is very common to encounter missing key point coordinates of visually occluded body parts in the output of OpenPose. To address this issue, a custom algorithm was used on the body key points identified for each person (JSON files) (see Fig. 4). Erroneous coordinates for a given key point were defined a priori as those that had an OpenPose confidence level less than 0.50. In our dataset, only 0.29% of the frames contained erroneous values for at least one body part. Linear interpolation was used for all the erroneous coordinates by fitting separate linear

```

# Algorithm for assigning unique IDs to all the people in the videos
Do for all videos
  Assign '0' id to the first person, '1' to the second and so on based on
  the first frame
  Update the person ID in the JSON file of the first frame
  Do for all frames
    Load data of all previous frames and the current frame
    Do for the last 5 frames
      Do for all the people present in the frame
        Store the data of the people into a variable for all
        people in the last 5 frames
    # Compare the data of people in the current frame with the
    people in the last 5 frames
    Do for all the people in the current frame
      Find the closest people from the previous frames by
      comparing the distances with the centroid of the body
      Compare the distances with other people in the frame
      Assign a new ID when a new person is found
      Update the person ID in the JSON file

```

Fig. 3. Algorithm for assigning unique IDs to all the people in the videos of a project.

functions for each missing interval. This step ensures that all face body key points were present throughout the video which is crucial for proper face tracking and eventually blurring. In the GUI, users have the option to choose between “interpolating only face coordinates” or “interpolating the coordinates of the whole body”. Interpolating only face coordinates is significantly faster, taking just 20.8% of the time required for whole-body interpolation. This option is suitable for users who are either solely interested in blurring their faces or prefer non-interpolated body kinematics. On the other hand, interpolating the kinematics of the entire body takes more time and is suitable for applications where linearly interpolated kinematics are required for further analysis (e.g., [85], [86]). In addition, SecurePose also saves non-interpolated body kinematics of the whole body (including the face) in the output folder, allowing users to use raw body coordinates for their application.

```

# Algorithm for interpolating the missing coordinates
Do for all videos
  Do for all people in the video
    Do for all the body key points (or only face points)
      Scan for the erroneous and missing frames (bad frames)
      Define a function for linear interpolation for each interval
      of bad frames
      Replace the wrong and missing values with the
      interpolated values
      Update the JSON file of the frames

```

Fig. 4. Algorithm for interpolating the missing coordinates of body key points.

I. Patient identification

Though it is valuable to track all the people throughout a video, for clinical purposes, the most important individual to identify is the patient. There are multiple possible ways to automate patient identification, including a deep learning approach, activity-specific movement recognition, and a rule-based approach to find the primary subject (focus) of the video. Deep learning and activity-specific movement recognition demand extensive training on vast datasets, yet they can falter

in practical scenarios, such as when patients exhibit minor or no movement abnormalities, or when someone other than the patient performs the same activity. Hence, we have adopted an approach that identifies a person as a patient based on their prominence in the video recording. Firstly, the movements of the body centroid for all individuals (each assigned a unique ID) in the video were tracked. Individuals who appeared in less than 80% of the frames were disregarded by assuming that in clinically relevant video patient stays in the field of the view of the camera in at least 80% the video’s duration. Subsequently, the average Euclidean distance between the body centroid and the center of the video frame was computed for each remaining person across all frames. The algorithm identifies the individual with the smallest average Euclidean distance to the center of the video frame as the primary subject (i.e. patient) in the clinical videos.

J. Blurring

A Python script is utilized to blur the faces of individuals within the video. Initially, the script reads the facial coordinates of body key points from the JSON files for each individual, separately. The centroid of these coordinates is then computed by taking the median values in the X and Y directions. Median values are used instead of mean to handle outliers effectively. Given that people with cerebral palsy can exhibit high-amplitude head movements, accurately estimating the face dimensions becomes challenging. Additionally, frames may contain small faces, and even a slight percentage error in face estimation can lead to compromise anonymity. To address this issue, face dimensions are estimated based on the length of the spine, which is defined as the distance between the neck and pelvis body key points. Leveraging the concept of human body proportions, the length of the face is assumed to be equal to one-third of the length of the spine [87]. For the sake of simplicity, the length and width of the face are assumed to be equal. To perform face blurring, the GUI provides multiple options. Users can select and apply person-specific blurring (patient only vs. all individuals) and choose the desired blurring types (Gaussian or solid) through the GUI.

K. Quality check

After completing the automated blurring, the GUI prompts an interactive window for assessing the quality of the blurring and improving it if required. The GUI allows the user to navigate across the videos and frames to find errors in blurring. After identifying these errors, the users can use the GUI to de-blur these frames or manually select the face regions to be blurred.

L. Export data

A window in the menu bar is designed to selectively export the project data to an external directory. Users can export the blurred videos, project back-up files, and coordinates of body key points (as JSON, CSV, or python variables).

M. System specifications

For analysis, a system having the following specifications was used: IntelR Core™ i9 12900 CPU @ 2.40 GHz 16 cores, 32-GB RAM, NVIDIA GeForce RTX3080 GPU with 10GB memory, 64-bit Windows 10 Operating System, and MATLAB 2022b platform. Other hardware and system requirements are mentioned in the software documentation [78].

N. Effect of face blurring on body key point extraction

To understand the effect of face blurring on body key point extraction accuracy, extracted coordinates were compared between blurred and pre-blurred videos. First, the coordinates of body key points from the 116 pre-blurred videos were extracted using SecurePose’s kinematic extraction pipeline. Then, the coordinates of body key points from manually face-blurred videos (not using SecurePose; details of manual blurring are described in the next section) were extracted using the same SecurePose pipeline. For this analysis, the coordinates extracted from pre-blurred videos were considered to be accurate, and any differences of the coordinates between blurred and pre-blurred videos were considered as errors due to blurring (calculated as the Euclidean distances between coordinates from pre-blurred and blurred videos). In addition, the confidence levels of estimation for each body key point were calculated for pre-blurred and blurred videos.

O. Comparison with six existing face blurring techniques

We compared the performance of SecurePose with six widely used face detection methods using our clinically-acquired video dataset. The trained models used and the reason for selection for each face detection method are shown in Table I. Since person-specific blurring is not possible using the six existing face blurring methods, SecurePose was used with “all person blurring” settings for this analysis. In other words, the faces of all individuals present in the video were blurred for this comparison.

TABLE I
SELECTED EXISTING METHODS FOR THE COMPARISON.

Model name	Original Article	Download link for trained model	Reason to select
VJ	[31]	[88]	Fastest and accurate face detector
HOG-based	[32]	[89]	Very low computational cost and more accurate than the VJ
MMOD	[53]	[90]	Outperformed contemporary methods on the Face Detection Data Set and Benchmark (FDDB) challenge
MTCNN	[54]	[91]	Outperformed contemporary methods on FDDB and WIDER Face. But computationally expensive.
YOLO-face	[65]	[92]	Outperformed contemporary methods on FDDB and WIDER Face. One of the fastest methods.
S3FD	[67]	[93]	Outperformed contemporary methods on AFW, PASCAL face, FDDB and WIDER Face.

All methods were compared against manual face blurring: 116 videos of people with cerebral palsy taken as they were walking (data set described above) were manually blurred by an experienced clinical researcher using Shotcut, an open-source video editing software [94]. The veracity of this manual face blurring was independently confirmed by another experienced clinical researcher, frame-by-frame.

All seven automated face blurring methods (including SecurePose and the selected six existing methods) were compared to manual face blurring (ground truth) for face detection performance in the 116 video dataset frame-by-frame (19753 frames in total). Intersection over union (IoU) was calculated for all the detected faces and the ground truth by using Eq. 1, where A_m is the region of the image marked as a face by the manual blurring, and A_d is the region of the image detected as a face by the algorithm. IoU of greater than or equal to 0.5 was considered as correctly detected face.

$$IoU = \frac{A_d \cap A_m}{A_d \cup A_m} \quad (1)$$

Automated methods were evaluated for:

- 1) True Positives (TP): A correct detection of ground truth face region. ($IoU \geq 0.5$ for ground truth face region)
- 2) False Positives (FP): An incorrect or a misplaced detection of a face region. ($IoU < 0.5$ for detected face regions)
- 3) False Negatives (FN): An undetected face region. ($IoU < 0.5$ for ground truth face regions)

In the context of face detection, the concept of true negatives (TN) doesn’t apply. This is because there is an infinite number of regions representing areas without faces within any given frame [95].

TP, FP, and FN were used to determine:

- 1) Precision: Precision is the ability of a model, when it detects a face, to have only detected ground truth face regions. A high precision value indicates that the model is able to accurately identify faces in an image without falsely detecting non-faces (see Eq. 2).

$$Precision = \frac{TP}{TP + FP} = \frac{TP}{All\ detections} \quad (2)$$

- 2) Recall: Recall is the ability of a model to detect all ground truth face regions. A high recall value indicates that the model is able to detect most of the faces in an image (see Eq. 3).

$$Recall = \frac{TP}{TP + FN} = \frac{TP}{All\ ground\ truths} \quad (3)$$

- 3) F1-score: F1-score can be interpreted as a measure of overall model performance from 0 to 1, where 1 is the best. The F1-score can be interpreted as the model's balanced ability to both capture positive cases (recall) and be accurate with the cases it does capture (precision) (see Eq. 4).

$$F1 - score = \frac{(2 * Precision * Recall)}{(Precision + Recall)} \quad (4)$$

- 4) Precision-recall curve: The method used in PASCAL VOC 2012 challenge [96] was used to calculate precision-recall characteristics. Since both the VJ and the MMOD do not provide confidence levels for their detections, a crucial element for computing precision-recall characteristics, the precision-recall characteristic was not calculated for these methods.
- 5) Average precision (AP): As described in the PASCAL VOC 2012 challenge [96] 11-point interpolation was used to calculate AP.

P. System Usability Scale (SUS)

To determine the usability of SecurePose in clinical and research settings, ten clinical researchers underwent a training session on how to use the software (~10 minutes), then asked to use the software, and ultimately give feedback on a System Usability Scale (SUS) [97]. The SUS is a well-established tool to assess the utility of software interfaces. It consists of ten questionnaire items (Table VI) on the Likert scale (1 to 5, strongly disagree to strongly agree) with variable weighting for each question [97]. The score ranges from 0 to 100, with an average score of 68 across all software products tested in the published literature. A score greater than 80.3 represents the top 10 percentile in usability of software products in the published literature [98]. The clinical researchers had different professional backgrounds (five with experience in gait analyses and clinical video analyses, three with experience in clinical video analysis, and two without any experience in gait or clinical video analysis) which allowed for a diverse range of experiences when assessing software usability.

III. RESULTS

A. Effect of face blurring on body key point extraction

To evaluate the effect of blurring on body key point coordinate extraction, two evaluation metrics were considered (discussed in Section II-N): 1) confidence level (generated for each set of x, y coordinates by OpenPose), and 2) error (the Euclidean distance between the coordinates for each body key point generated by OpenPose pre-face blurring vs post-face blurring).

Table II shows the mean confidence level for each key body point in pre-blurred and blurred videos across all frames and the mean error in coordinates extracted from the face-blurred videos. The results show that the confidence level for all body key points significantly decreased after blurring (p-value < 0.05, one-way ANOVA) and were particularly low (< 0.75) for points adjacent to the blurred face (shoulders and chest). Notably, all body key points extracted from blurred videos had different coordinates than body key points extracted from unblurred videos (i.e. blurring caused errors in extraction of all body key points).

TABLE II
MEAN CONFIDENCE LEVEL FOR COORDINATES EXTRACTION IN PRE-BLURRED AND BLURRED VIDEOS, AND MEAN ABSOLUTE ERROR FOR COORDINATES EXTRACTION IN BLURRED VIDEOS.

Body key point	Confidence level (pre-blurred)	Confidence level (blurred)	Error (pixel)
0	0.868	0.315	14
1	0.890	0.692	8
2	0.891	0.708	7
3	0.920	0.905	4
4	0.940	0.934	3
5	0.893	0.710	8
6	0.908	0.895	4
7	0.899	0.892	3
8	0.948	0.934	3
9	0.887	0.866	3
10	0.930	0.910	4
11	0.866	0.844	4
12	0.852	0.840	5
13	0.891	0.889	4
14	0.886	0.872	4
15	0.861	0.309	16
16	0.881	0.310	15
17	0.847	0.250	16
18	0.848	0.211	17
19	0.882	0.764	4
20	0.859	0.803	4
21	0.846	0.769	5
22	0.856	0.791	5
23	0.849	0.834	3
24	0.834	0.829	4

Though OpenPose cannot reliably track individuals across frames in a video, it should be able to differentiate between individuals and their associated key point coordinates within the same frame. After blurring, there were instances of OpenPose associating key point coordinates with the incorrect individual in a given frame (see Fig. 5). Additionally, there were instances of OpenPose confusing left and right body parts in the blurred video samples (see Fig. 5). These observations indicate the need to perform coordinate extraction before blurring the videos to get accurate readings.

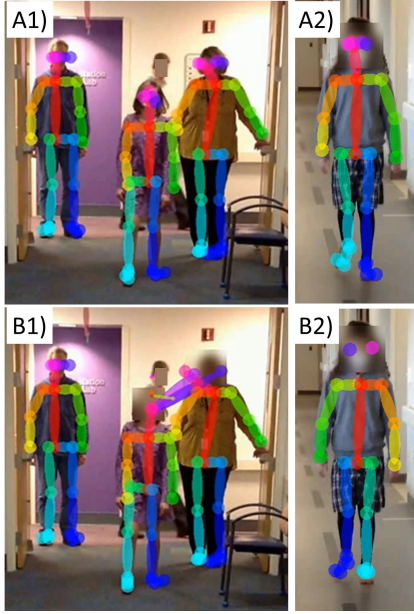


Fig. 5. Examples where kinematic extraction failed in blurred videos. A1 and A2 and the results of kinematic extraction on pre-blurred videos, and B1 and B2 are the results of kinematic extraction on blurred videos. B1) Openpose failed to differentiate between individuals and their associated key point coordinates within the same frame. B2) OpenPose wrongly associated left and right body parts in the blurred video.

B. Automatic face detection

The performance comparison of methods is presented in Table III, Fig. 6 and Fig. 7. Table III shows that SecurePose and three of the six selected existing methods had precision > 0.9 , i.e., when they detected a face, there was a high likelihood of a ground truth face detection. The lowest precision was for the HOG-based detector at 0.689. Though some existing methods had comparable precision to SecurePose, none had comparable recall. That is, all six selected existing methods had a low ability to detect all ground truth face regions with recall ranging from 0.282-0.588. Examples of blurring errors committed by SecurePose and the other six assessed methods are shown in Fig. 8.

SecurePose emerged as the standout method, achieving high values in both precision and recall (precision: 0.992, recall: 0.990, F1-score: 0.991), demonstrating its proficiency in accurately and reliably detecting faces within a frame. Furthermore, SecurePose exhibited superior precision-recall characteristics, surpassing other methods and excelling in terms of average precision (AP = 0.948) (see Table III, Fig. 6 and Fig. 7). These results suggest that SecurePose provides better face detection than the six selected existing methods on clinically recorded gait videos.

TABLE III
PRECISION, RECALL, F1-SCORE AND AVERAGE PRECISION (AP) FOR THE SIX SELECTED EXISTING METHODS AND SECUREPOSE

Methods	Precision	Recall	F1-score	AP
Viola Jones	0.937	0.488	0.642	-
HOG-based detector	0.689	0.282	0.400	0.243
MMOD	0.822	0.376	0.516	-
MTCNN	0.850	0.579	0.689	0.534
YOLO-face	0.956	0.588	0.728	0.543
S ³ FD	0.935	0.580	0.716	0.540
SecurePose	0.992	0.990	0.991	0.948

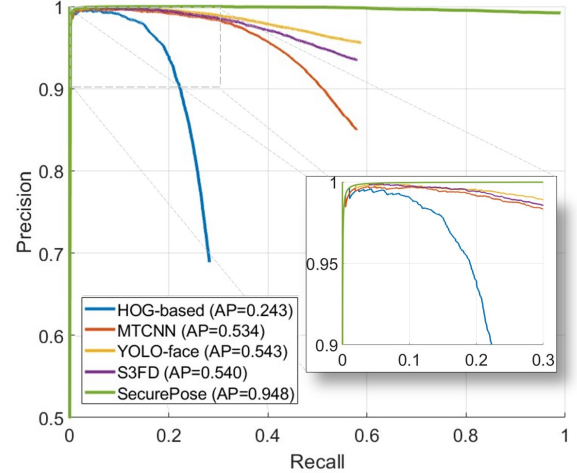


Fig. 6. Precision-recall curve with average precision values for SecurePose and selected existing methods.

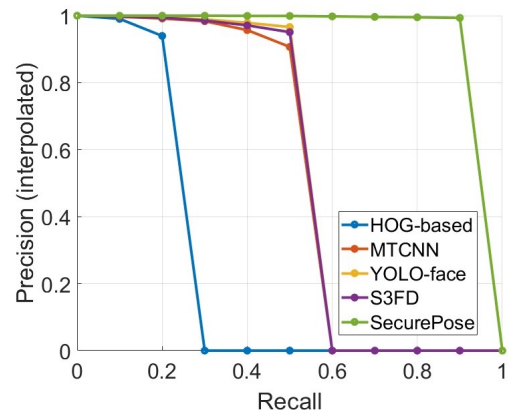


Fig. 7. 11 points interpolated precision-recall curve for SecurePose and selected existing methods.

Table IV illustrates the comparison of methods in terms of computational costs. Viola Jones emerged as the fastest method, followed by SecurePose. SecurePose demonstrated efficiency by utilizing minimal CPU, RAM, and GPU resources, albeit with higher disk usage compared to other methods. Overall, the results suggest that SecurePose is fast and uses less CPU, RAM, and GPU resources than all other methods assessed.

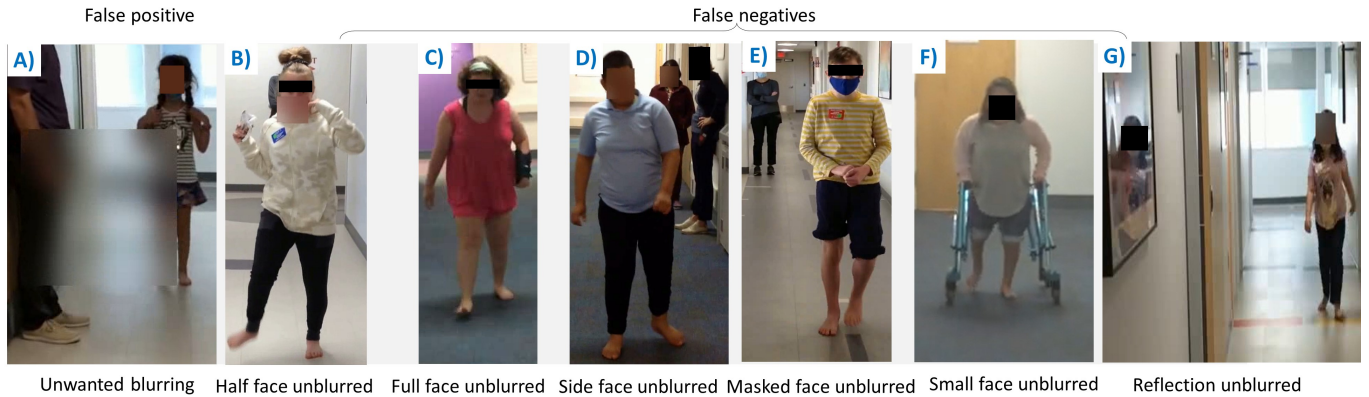


Fig. 8. Examples of some commonly observed failure cases in automated blurring, A) unwanted blurring (Viola Jones), B) half-face unblurred (HOG-based detector), C) full-face unblurred (MTCNN), D) side-face unblurred (ResNet), E) masked-face unblurred (YOLO-face), F) small-face unblurred (S³FD and G) unblurred face in reflection (SecurePose). The unblurred face regions are masked with a black patch to hide the identities.

TABLE IV
COMPUTATIONAL COST OF USING THE METHODS WITH THE SYSTEM SPECIFICATIONS MENTIONED IN THE SECTION II-M.

Methods	Computational time (minutes)	CPU (%)	RAM (GB)	GPU (%)	GPU-memory (GB)	Disk-SSD (MB/s)
Viola Jones	25	48	0.351	NA	NA	0.1
HOG-based detector	42	9	0.145	NA	NA	0.9
MMOD	7936	10	1.942	NA	NA	0.1
MTCNN	153	8	0.390	26	8,600	0.1
YOLO-face	66	60	0.259	NA	NA	0.3
S ³ FD	334	58	0.331	NA	NA	0.1
SecurePose	35	8	0.113	NA	0.105	2.5

C. Person tracking and identification

Though the person tracking and identification strategy used by SecurePose likely contributed to higher precision, recall, F1-score and AP than other existing methods, this methodology had its own limitations. In 110 out of 116 videos (94.8%), the algorithms successfully tracked and assigned unique IDs to all the individuals in the videos. In 3 videos (2.6%), the unique IDs of two individuals (both non-patient) were interchanged 1-2 times. Since these people were standing very close in a line, their body centroids collided. Also, as the person in the front was blocking more than 80% of the body of the other person, it became difficult for the algorithm to differentiate between these people. In the remaining 3 videos (2.6%), the algorithm could not assign a unique ID to non-patient individuals because their bodies were largely occluded. However, these issues did not affect face blurring of these individuals in any of the videos.

D. Patient identification

The algorithm employed for patient identification operated under the assumption that the individual closest to the frame's center would be the focus of the video recording (the patient). The assumption held true in all other videos, yielding a 99% (115 out of 116) success rate for patient identification across

the dataset. However, this assumption proved erroneous in a single video where a caregiver accompanied the patient throughout the recording. Consequently, the algorithm incorrectly labeled the caregiver as the patient in that instance.

These relatively rare errors provide valuable user guidance for the implementation of SecurePose e.g., added caution regarding the patient-specific face blurring when there are other individuals in the center of the video (e.g. another person assisting the patient). In these cases, it would be best to use the "all person blurring" settings of SecurePose.

E. Improvements after quality check

After automated face blurring, a manual quality check was performed. The manual quality checking achieved ceiling performance with an added time of 48 minutes for all 116 videos in aggregate (25 seconds/video). Compared to the time required for ground truth blurring, SecurePose obtained the same performance in less manual effort and time (8.92% of the time taken to blur the videos manually). Please refer to Table V for more details of the performance comparison.

TABLE V
PRECISION, RECALL, F1-SCORE AND TOTAL TIME TAKEN BY SECUREPOSE AUTOMATICS BLURRING AND SECUREPOSE WITH MANUAL QUALITY CHECK ARE SHOWN IN THE TABLE. ALSO, THE TABLE INCLUDES THE TOTAL TIME TAKEN BY GROUND TRUTH MANUAL BLURRING.

Blurring stages	Precision	Recall	F1- score	Time (minutes)
Automated blurring	0.992	0.990	0.991	35
After manual quality check	1.000	1.000	1.000	83
Manual Blurring	NA	NA	NA	930

F. System Usability Scale (SUS) results

The average SUS score across these 10 users was 88.75, indicating a high percentile ranking in usability when compared to other software products assessed using the SUS in the literature [98] (Table VI).

TABLE VI
SYSTEM USABILITY SCALE (SUS) SCORE

S.No.	Questionnaire items	Average of responses	Score contribution
1	I think that I would like to use this software frequently	3.8	2.8
2	I found the software unnecessarily complex	1.9	3.1
3	I thought the software was easy to use	4.8	3.8
4	I think that I would need the support of a technical person to be able to use this software	1.2	3.8
5	I found that various functions in this software were well integrated	4.8	3.8
6	I thought there was too much inconsistency in this software	1.0	4.0
7	I would imagine that most people would learn to use this software very quickly	4.8	3.8
8	I found the software very cumbersome to use	2.2	2.8
9	I felt very confident using the software	4.8	3.8
10	I need to learn a lot of things before I could get going with this software	1.2	3.8
Sum			35.5

Average SUS score = 88.75 (35.5*2.5)

IV. DISCUSSION

We have developed a face blurring algorithm called SecurePose that, when compared against six existing face blurring methodologies, is the best performing face blurring method for use in clinically acquired video data sets. With only a fraction of the time required for ground truth manual blurring, SecurePose can achieve identical performance following quality check steps. This is a significant step forward for the rapid blurring and de-identified sharing and analysis of clinically acquired video data sets.

SecurePose has better precision, recall, F1-score and average precision for face blurring of the patient in clinical videos than six existing face detection methods while maintaining a high usability rating from clinical researchers. Additionally, the software enables the extraction and export of comprehensive full-body kinematics data for subsequent analysis without losing the extraction quality by performing the extraction prior to face blurring. The automated patient kinematics extraction capability of the software has the potential to facilitate clinical assessment and accelerate research in movement disorders.

Person tracking and patient identification algorithms were used to facilitate accurate and automated patient body kinematic extraction. Notably, it achieved a 94.8% success rate in the person tracking and a 99% success rate in the patient identification. The validation results illustrated that SecurePose can perform person-specific face blurring in the vast majority of clinical gait videos. It is additionally notable that this testing occurred on a clinically-relevant data set using videos recorded on a handheld iPad (thus subject to issues with motion, focus, and illumination). The videos of the patients were recorded during a busy clinic (many of whom had masks or clothing covering body key points, thus complicating kinematics extraction and face identification). This real-world data set makes the high performance of SecurePose even more valuable.

A. Limitations and future work

SecurePose was validated for face blurring and body kinematic extraction on a clinically relevant gait examination. However, it is necessary to extend the validation of SecurePose to other clinically relevant video-based assessments, such as during seated or recumbent tasks or during other exam maneuvers. Since the primary objective of this study was to develop

reliable software for clinical applications, the algorithms were not optimized for reducing computational time. In the future, multi-threading and optimized algorithms will be used to reduce the automated kinematics extraction and face blurring time. The algorithms developed for person tracking, person identification and patient identification were designed for fast and accurate clinical applications. However, these algorithms may not work as expected in non-clinical applications. In the future, the software will be modified to perform face blurring in non-clinical applications. The patient identification algorithm used a rule-based approach that assumes the presence of the patient in the video for more than 80% of the video's duration and that the patient remains close to the center throughout the video. This approach worked correctly in 99% of the gait videos. However, we would need different rules for activities where these assumptions may not logically remain true. The current version of the software works only on a local server. This approach ensures the privacy of the patient data but demands a local server with high computational power. A web-based application would be valuable to allow cloud computing for automated kinematics extraction and face blurring, thus improving accessibility across institutions.

V. CONCLUSION

This paper presents the development and validation of open-source software named "SecurePose" for automated face blurring and human kinematic extraction in clinically recorded gait videos. SecurePose obtained a precision of 0.992, recall of 0.990, F1-score of 0.991 and average precision of 0.948 on 116 gait videos of people with cerebral palsy in automated face detection. Also, it attained the same performance as the manual blurring method in 8.92% of the time. Experienced researchers found it user-friendly, confirming its usability on the System Usability Scale. This study affirms the software's efficacy, efficiency and usability for selective and non-selective face blurring and kinematic extraction in clinical gait videos.

REFERENCES

- [1] C. Einspieler and H. F. Prechtel, "Prechtel's assessment of general movements: a diagnostic tool for the functional assessment of the young nervous system," *Mental retardation and developmental disabilities research reviews*, vol. 11, no. 1, pp. 61–67, 2005.
- [2] C. L. Comella, S. Leurgans, J. Wu, G. T. Stebbins, T. Chmura, and D. S. Group, "Rating scales for dystonia: a multicenter assessment," *Movement disorders*, vol. 18, no. 3, pp. 303–312, 2003.

- [3] T. Brown and A. Lalor, "The movement assessment battery for children—second edition (mabc-2): a review and critique," *Physical & occupational therapy in pediatrics*, vol. 29, no. 1, pp. 86–103, 2009.
- [4] R. Bajpai and D. Joshi, "A-gas: A probabilistic approach for generating automated gait assessment score for cerebral palsy children," *IEEE Transactions on Neural Systems and Rehabilitation Engineering*, vol. 29, pp. 2530–2539, 2021.
- [5] A. Act, "Health insurance portability and accountability act of 1996," *Public law*, vol. 104, p. 191, 1996.
- [6] P. Regulation, "General data protection regulation," *Intouch*, vol. 25, pp. 1–5, 2018.
- [7] D. Prasad M and S. Menon C, "The personal data protection bill, 2018: India's regulatory journey towards a comprehensive data protection law," *International Journal of Law and Information Technology*, vol. 28, no. 1, pp. 1–19, 2020.
- [8] Z. Cao, T. Simon, S.-E. Wei, and Y. Sheikh, "Realtime multi-person 2d pose estimation using part affinity fields," in *Proceedings of the IEEE conference on computer vision and pattern recognition*, 2017, pp. 7291–7299.
- [9] [Online]. Available: <https://www.tensorflow.org/hub/tutorials/movenet/>
- [10] [Online]. Available: <https://github.com/google-coral/project-posenet/>
- [11] Z. Liu, H. Chen, R. Feng, S. Wu, S. Ji, B. Yang, and X. Wang, "Deep dual consecutive network for human pose estimation," in *Proceedings of the IEEE/CVF Conference on Computer Vision and Pattern Recognition (CVPR)*, June 2021, pp. 525–534.
- [12] R. A. Güler, N. Neverova, and I. Kokkinos, "Densepose: Dense human pose estimation in the wild," 2018.
- [13] J. Jiang, W. Skalli, A. Siadat, and L. Gajny, "Effect of face blurring on human pose estimation: Ensuring subject privacy for medical and occupational health applications," *Sensors*, vol. 22, no. 23, p. 9376, 2022.
- [14] A. Ali-Gombe, E. Elyan, and J. Zwiegelaar, "Towards a reliable face recognition system," in *Proceedings of the 21st EANN (Engineering Applications of Neural Networks) 2020 Conference: Proceedings of the EANN 2020 21*. Springer, 2020, pp. 304–316.
- [15] S. P. Otta, S. Kolipara, S. Panda, and C. Hota, "User identification with face recognition: A systematic analysis," in *2022 3rd International Conference for Emerging Technology (INCET)*. IEEE, 2022, pp. 1–6.
- [16] M. K. Hasan, M. S. Ahsan, S. S. Newaz, and G. M. Lee, "Human face detection techniques: A comprehensive review and future research directions," *Electronics*, vol. 10, no. 19, p. 2354, 2021.
- [17] M. Kass, A. Witkin, and D. Terzopoulos, "Snakes: Active contour models," *International journal of computer vision*, vol. 1, no. 4, pp. 321–331, 1988.
- [18] A. Nikolaidis and I. Pitas, "Facial feature extraction and pose determination," *Pattern Recognition*, vol. 33, no. 11, pp. 1783–1791, 2000.
- [19] C.-L. Huang and C.-W. Chen, "Human facial feature extraction for face interpretation and recognition," *Pattern recognition*, vol. 25, no. 12, pp. 1435–1444, 1992.
- [20] A. L. Yuille, P. W. Hallinan, and D. S. Cohen, "Feature extraction from faces using deformable templates," *International journal of computer vision*, vol. 8, pp. 99–111, 1992.
- [21] A. Lanitis, A. Hill, T. F. Cootes, and C. J. Taylor, "Locating facial features using genetic algorithms," in *International Conference on Digital Signal Processing*, 1995, pp. 520–525.
- [22] J. L. Crowley and F. Berard, "Multi-modal tracking of faces for video communications," in *Proceedings of IEEE Computer Society Conference on Computer Vision and Pattern Recognition*. IEEE, 1997, pp. 640–645.
- [23] S. McKenna, S. Gong, and H. Liddell, "Real-time tracking for an integrated face recognition system," in *Second European Workshop on Parallel Modelling of Neural Operators*, vol. 11, 1995.
- [24] J. Kovac, P. Peer, and F. Solina, *Human skin color clustering for face detection*. IEEE, 2003, vol. 2.
- [25] H. P. Graf, E. Cosatto, D. Gibbon, M. Kocheisen, and E. Petajan, "Multi-modal system for locating heads and faces," in *Proceedings of the Second International Conference on Automatic Face and Gesture Recognition*. IEEE, 1996, pp. 88–93.
- [26] G. Guo, S. Z. Li, and K. L. Chan, "Support vector machines for face recognition," *Image and Vision computing*, vol. 19, no. 9–10, pp. 631–638, 2001.
- [27] N. Ahmed, T. Natarajan, and K. R. Rao, "Discrete cosine transform," *IEEE transactions on Computers*, vol. 100, no. 1, pp. 90–93, 1974.
- [28] A. R. Chadha, P. P. Vaidya, and M. M. Roja, "Face recognition using discrete cosine transform for global and local features," in *2011 International Conference On Recent Advancements In Electrical, Electronics And Control Engineering*. IEEE, 2011, pp. 502–505.
- [29] X. He and P. Niyogi, "Locality preserving projections," *Advances in neural information processing systems*, vol. 16, 2003.
- [30] J. Héroult, "Réseaux de neurones à synapses modifiables: Décodage de messages sensoriels composites par une apprentissage non supervisé et permanent," *CR Acad. Sci. Paris*, pp. 525–528, 1984.
- [31] P. Viola and M. Jones, "Rapid object detection using a boosted cascade of simple features," in *Proceedings of the 2001 IEEE computer society conference on computer vision and pattern recognition. CVPR 2001*, vol. 1. Ieee, 2001, pp. 1–I.
- [32] N. Dalal and B. Triggs, "Histograms of oriented gradients for human detection," in *2005 IEEE computer society conference on computer vision and pattern recognition (CVPR'05)*, vol. 1. Ieee, 2005, pp. 886–893.
- [33] A. Devaux, N. Paparoditis, F. Precioso, and B. Cannelle, "Face blurring for privacy in street-level geoviewers combining face, body and skin detectors," in *MVA*, 2009, pp. 86–89.
- [34] K. Brkić, T. Hrkać, Z. Kalafatić, and I. Sikirić, "Face, hairstyle and clothing colour de-identification in video sequences," *IET Signal Processing*, vol. 11, no. 9, pp. 1062–1068, 2017.
- [35] Z. Liu, M. Hao, and Y. Hu, "Visual anonymity: Automated human face blurring for privacy-preserving digital videos."
- [36] F. S. Al-Mukhtar, "Tracking and blurring the face in a video file," *Al-Nahrain Journal of Science*, no. 1, pp. 202–207, 2018.
- [37] Y. Pang, Y. Yuan, X. Li, and J. Pan, "Efficient hog human detection," *Signal processing*, vol. 91, no. 4, pp. 773–781, 2011.
- [38] A. Adouani, W. M. B. Henia, and Z. Lachiri, "Comparison of haar-like, hog and lbp approaches for face detection in video sequences," in *2019 16th International Multi-Conference on Systems, Signals & Devices (SSD)*. IEEE, 2019, pp. 266–271.
- [39] C. Rahmad, R. A. Asmara, D. Putra, I. Dharma, H. Darmono, and I. Muhiqqin, "Comparison of viola-jones haar cascade classifier and histogram of oriented gradients (hog) for face detection," in *IOP conference series: materials science and engineering*, vol. 732, no. 1. IOP Publishing, 2020, p. 012038.
- [40] H. A. Rowley, S. Baluja, and T. Kanade, "Neural network-based face detection," *IEEE Transactions on pattern analysis and machine intelligence*, vol. 20, no. 1, pp. 23–38, 1998.
- [41] K. Steinbuch and U. A. Piske, "Learning matrices and their applications," *IEEE Transactions on Electronic Computers*, no. 6, pp. 846–862, 1963.
- [42] D. E. Rumelhart, G. E. Hinton, and R. J. Williams, "Learning representations by back-propagating errors," *nature*, vol. 323, no. 6088, pp. 533–536, 1986.
- [43] M. J. Orr *et al.*, "Introduction to radial basis function networks," 1996.
- [44] S.-Y. Kung, S.-H. Lin, and M. Fang, "A neural network approach to face/palm recognition," in *Proceedings of 1995 IEEE Workshop on Neural Networks for Signal Processing*. IEEE, 1995, pp. 323–332.
- [45] M. Turk and A. Pentland, "Eigenfaces for recognition," *Journal of cognitive neuroscience*, vol. 3, no. 1, pp. 71–86, 1991.
- [46] L. Sirovich and M. Kirby, "Low-dimensional procedure for the characterization of human faces," *Josa a*, vol. 4, no. 3, pp. 519–524, 1987.
- [47] M. A. Turk and A. P. Pentland, "Face recognition using eigenfaces," in *Proceedings. 1991 IEEE computer society conference on computer vision and pattern recognition*. IEEE Computer Society, 1991, pp. 586–587.
- [48] B. Moghaddam and A. Pentland, "Probabilistic visual learning for object detection," in *Proceedings of IEEE international conference on computer vision*. IEEE, 1995, pp. 786–793.
- [49] P. N. Belhumeur, J. P. Hespanha, and D. J. Kriegman, "Eigenfaces vs. fisherfaces: Recognition using class specific linear projection," *IEEE Transactions on pattern analysis and machine intelligence*, vol. 19, no. 7, pp. 711–720, 1997.
- [50] K. Pearson, "Liii. on lines and planes of closest fit to systems of points in space," *The London, Edinburgh, and Dublin philosophical magazine and journal of science*, vol. 2, no. 11, pp. 559–572, 1901.
- [51] H. Hotelling, "Analysis of a complex of statistical variables into principal components," *Journal of educational psychology*, vol. 24, no. 6, p. 417, 1933.
- [52] V. N. Vapnik, "Pattern recognition using generalized portrait method," *Automation and remote control*, vol. 24, no. 6, pp. 774–780, 1963.
- [53] D. E. King, "Max-margin object detection," *arXiv preprint arXiv:1502.00046*, 2015.
- [54] K. Zhang, Z. Zhang, Z. Li, and Y. Qiao, "Joint face detection and alignment using multitask cascaded convolutional networks," *IEEE Signal Processing Letters*, vol. 23, no. 10, pp. 1499–1503, 2016.
- [55] X. Zhu and D. Ramanan, "Face detection, pose estimation, and landmark localization in the wild," in *2012 IEEE conference on computer vision and pattern recognition*. IEEE, 2012, pp. 2879–2886.

- [56] J. Prinosil and O. Maly, "Detecting faces with face masks," in *2021 44th International Conference on Telecommunications and Signal Processing (TSP)*. IEEE, 2021, pp. 259–262.
- [57] T. Edirisooriya and E. Jayatunga, "Comparative study of face detection methods for robust face recognition systems," in *2021 5th SLAAI International Conference on Artificial Intelligence (SLAAI-ICAI)*. IEEE, 2021, pp. 1–6.
- [58] J. Zhou, C.-M. Pun, and Y. Wang, "Pixelation is not done in videos yet," *arXiv preprint arXiv:1903.10836*, 2019.
- [59] T. Park, N. P. Phu, and H. Kim, "Cnn based face tracking and re-identification for privacy protection in video contents," *Journal of the Korea Information and Communications Society*, vol. 25, no. 1, pp. 63–68, 2021.
- [60] Y. Su and X. Liu, "Front view gait (fvg-b) database," 2022.
- [61] X. Wei and Q. Yin, "Comparison and application of two face detection algorithms," in *Proceedings of the 5th International Conference on Signal Processing and Information Communications*. Springer, 2022, pp. 53–62.
- [62] S. Ren, K. He, R. Girshick, and J. Sun, "Faster r-cnn: Towards real-time object detection with region proposal networks," *Advances in neural information processing systems*, vol. 28, 2015.
- [63] W. Liu, D. Anguelov, D. Erhan, C. Szegedy, S. Reed, C.-Y. Fu, and A. C. Berg, "Ssd: Single shot multibox detector," in *Computer Vision—ECCV 2016: 14th European Conference, Amsterdam, The Netherlands, October 11–14, 2016, Proceedings, Part I 14*. Springer, 2016, pp. 21–37.
- [64] J. Redmon and A. Farhadi, "Yolov3: An incremental improvement," *arXiv*, 2018.
- [65] W. Chen, H. Huang, S. Peng, C. Zhou, and C. Zhang, "Yolo-face: a real-time face detector," *The Visual Computer*, vol. 37, pp. 805–813, 2021.
- [66] K. Kim, Z. Yang, I. Masi, R. Nevatia, and G. Medioni, "Face and body association for video-based face recognition," in *2018 IEEE Winter Conference on Applications of Computer Vision (WACV)*. IEEE, 2018, pp. 39–48.
- [67] S. Zhang, X. Zhu, Z. Lei, H. Shi, X. Wang, and S. Z. Li, "S3fd: Single shot scale-invariant face detector," in *Proceedings of the IEEE international conference on computer vision*, 2017, pp. 192–201.
- [68] A. Meethal, M. Pedersoli, S. Belharbi, and E. Granger, "Convolutional sn for weakly supervised object localization," in *2020 25th International Conference on Pattern Recognition (ICPR)*. IEEE, 2021, pp. 10 157–10 164.
- [69] P. Hu and D. Ramanan, "Finding tiny faces," in *Proceedings of the IEEE conference on computer vision and pattern recognition*, 2017, pp. 951–959.
- [70] S. Yang, P. Luo, C. C. Loy, and X. Tang, "Faceness-net: Face detection through deep facial part responses," *IEEE transactions on pattern analysis and machine intelligence*, vol. 40, no. 8, pp. 1845–1859, 2017.
- [71] R. Ranjan, V. M. Patel, and R. Chellappa, "A deep pyramid deformable part model for face detection," in *2015 IEEE 7th international conference on biometrics theory, applications and systems (BTAS)*. IEEE, 2015, pp. 1–8.
- [72] Z. Yang and R. Nevatia, "A multi-scale cascade fully convolutional network face detector," in *2016 23rd International Conference on Pattern Recognition (ICPR)*. IEEE, 2016, pp. 633–638.
- [73] M. Mathias, R. Benenson, M. Pedersoli, and L. Van Gool, "Face detection without bells and whistles," in *Computer Vision—ECCV 2014: 13th European Conference, Zurich, Switzerland, September 6–12, 2014, Proceedings, Part IV 13*. Springer, 2014, pp. 720–735.
- [74] S. Mroz, N. Baddour, C. McGuirk, P. Juneau, A. Tu, K. Cheung, and E. Lemaire, "Comparing the quality of human pose estimation with blazepose or openpose," in *2021 4th International Conference on Bio-Engineering for Smart Technologies (BioSMART)*. IEEE, 2021, pp. 1–4.
- [75] J. Stenum, C. Rossi, and R. T. Roemmich, "Two-dimensional video-based analysis of human gait using pose estimation," *PLoS computational biology*, vol. 17, no. 4, p. e1008935, 2021.
- [76] B. Zhu, H. Fang, Y. Sui, and L. Li, "Deepfakes for medical video de-identification: Privacy protection and diagnostic information preservation," in *Proceedings of the AAAI/ACM Conference on AI, Ethics, and Society*, 2020, pp. 414–420.
- [77] A. Kumar, A. Kaur, and M. Kumar, "Face detection techniques: a review," *Artificial Intelligence Review*, vol. 52, pp. 927–948, 2019.
- [78] [Online]. Available: <https://sourceforge.net/projects/securepose/>
- [79] [Online]. Available: https://www.youtube.com/playlist?list=PLO4_jCYO5Ib23MoBpn-Wpj1_b6DAYIDwk
- [80] P. Rosenbaum, N. Paneth, A. Leviton, M. Goldstein, M. Bax, D. Damiano, B. Dan, B. Jacobsson *et al.*, "A report: the definition and classification of cerebral palsy april 2006," *Dev Med Child Neurol Suppl*, vol. 109, no. suppl 109, pp. 8–14, 2007.
- [81] D. J. Russell, P. Rosenbaum, M. Wright, and L. M. Avery, *Gross motor function measure (GMFM-66 & GMFM-88) users manual*. Mac Keith press, 2002.
- [82] R. Palisano, P. Rosenbaum, S. Walter, D. Russell, E. Wood, and B. Galuppi, "Development and reliability of a system to classify gross motor function in children with cerebral palsy," *Developmental medicine & child neurology*, vol. 39, no. 4, pp. 214–223, 1997.
- [83] F. Lundh, "An introduction to tkinter," *URL: www.pythonware.com/library/tkinter/introduction/index.htm*, 1999.
- [84] G. Van Rossum, *The Python Library Reference, release 3.8.2*. Python Software Foundation, 2020.
- [85] C. M. O'Connor, S. K. Thorpe, M. J. O'Malley, and C. L. Vaughan, "Automatic detection of gait events using kinematic data," *Gait & posture*, vol. 25, no. 3, pp. 469–474, 2007.
- [86] R. Bajpai and D. Joshi, "Movenet: A deep neural network for joint profile prediction across variable walking speeds and slopes," *IEEE Transactions on Instrumentation and Measurement*, vol. 70, pp. 1–11, 2021.
- [87] L. K. Osterkamp, "Current perspective on assessment of human body proportions of relevance to amputees," *Journal of the American Dietetic Association*, vol. 95, no. 2, pp. 215–218, 1995.
- [88] [Online]. Available: https://github.com/opencv/opencv/blob/master/data/haarcascades/haarcascade_frontalface_default.xml
- [89] [Online]. Available: <https://pypi.org/project/dlib/>
- [90] [Online]. Available: https://github.com/davisking/dlib-models/blob/master/mmod_human_face_detector.dat.bz2
- [91] [Online]. Available: <https://pypi.org/project/mtcnn/>
- [92] [Online]. Available: <https://github.com/derronqi/yolov8-face>
- [93] [Online]. Available: <https://github.com/sfzhang15/SFD>
- [94] [Online]. Available: <https://www.shotcut.org/>
- [95] R. Padilla, S. L. Netto, and E. A. Da Silva, "A survey on performance metrics for object-detection algorithms," in *2020 international conference on systems, signals and image processing (IWSSIP)*. IEEE, 2020, pp. 237–242.
- [96] M. Everingham, L. Van Gool, C. K. Williams, J. Winn, and A. Zisserman, "The pascal visual object classes (voc) challenge," *International journal of computer vision*, vol. 88, pp. 303–338, 2010.
- [97] J. Brooke, "Sus: a 'quick and dirty' usability," *Usability evaluation in industry*, vol. 189, no. 3, pp. 189–194, 1996.
- [98] J. Sauro, *A practical guide to the system usability scale: Background, benchmarks & best practices*. Measuring Usability LLC, 2011.